Readiness of Stir Casting 6061 Al-Al_2O_3 Metal Matrix Composites and Investigation of Wear and Mechanical Properties

Balraj Hooda[1], Dishant Shokeen[2], Gaurav Kumar[3], Neeraj Prihar[4], Vivek Singh[5]

[1,2,3,4,5]Ganga Institute of Technology and Management, Kablana

ABSTRACT

The automotive, aerospace, and marine sectors favorsaluminum metal matrix composites (AMCs) over conventional materials due to its remarkable attributes, such as superior resilience to wear and a high solidarity to weight ratio. The current study's objective is to blend metal lattice composite utilizing the mix projecting technique from the fluid metallurgy course, with 6061Al serving as the network material and ceramic Al_2O_3 particles for support. From support expansion level is being changed in increments of wt.%. Support particles for each composite were heated to 2000C and then distributed in groups of three into the liquid Al6061 compound vortex to promote wettability and circulation. For the aforementioned pre-assembled composites, microstructural representation was carried out using samples from the central portion of the material to ensure uniform particle dispersion. When Al_2O_3 particles expand, the prearranged features of hardness and malleability are not fixed, thus it is important to monitor the extent of advancement. The samples exhibit a degree of grain refinement and really uniform conveyance, as shown by the microstructural characterization of the composites. Furthermore, as compared to an unreinforced 6061Al network, composites have superior hardness and tractable characteristics. Similarly, increasing the amount of support has caused further expansion in both rigidity and hardness.

Keywords: MMCs: Stir-casting machine, AA6061

INTRODUCTION

Because they contain small estimated support particles in the matrix, metal-grid composites (MMCs) are the most promising materials for achieving improved mechanical properties, such as hardness, Young's modulus, yield strength, and extreme rigidity [Vencl An et al., (2010) and Yung C.K et al., (2004)]. Because of their excellent mechanical and physical qualities, aluminum-framework composites (AMCs) constructed with broken fortifications are seeing increased usage in the automotive, military, aerospace, and power industries [Sajjadi SAet al., (2010), A.R.K. Swamy et al., (2011), and Ceschini L et al., (2006)]. Among Al-combinations, 6061Al-composite is widely used in designing sectors where common mechanical features like elasticity, hardness, and so forth are essentially needed, such as transportation and development [Vencl An et al., (2010) and Chawla Net al., (2001)]. To improve the characteristics of the 6061Al combination, a variety of materials are being used as fortifications, including SiC, Al_2O_3, B4C, TiB2, ZrO2, SiO2, and graphite. However, the automotive and aerospace industries are increasingly using Al_2O_3 or SiC molecule built up aluminum compound lattice composites for applications such as cylinders, chamber heads, connecting bars, and so forth where the materials' tribological qualities are crucial [Vencl An et al., (2010) and Sajjadi SA et al., (2011) and C.S. Ramesh et al., (2005)].

MMCs' mechanical characteristics are very sensitive to the handling method used. By advancing the handling approach using science-based exhibiting ways, significant improvements may be achieved. Powder metallurgy, liquefy strategies, and crush projecting are some of the techniques that have been used to set up the composites [Yung C.K et al., (2004), Sajjadi SA et al., (2010), and Sajjadi SA et al., (2010)]. Regardless, powder metallurgy appears to be the cycle of choice due to its ability to produce more uniform scatterings. In order to benefit from both applying compressive forces and high temperatures at the same time, hot expulsion is typically used as a post-treatment [Mazahery An et al., 2011].

Although fluid state management offers certain notable advantages, powder metallurgy produces MMCs with superior mechanical characteristics. According to Vencl An et al. (2010) and Chawla N et al. (2001), they are as follows: improved framework molecule holding, more simple management of grid structure, effortlessness, minimal handling expense, closer net shape, and the broad selection of materials. Two methods are used in the fluid state manufacturing of MMCs, and both depend on the temperature at which the particles are dissolved. Whereas the particles in the compo-projecting technique are integrated at the amalgam's semi-strong slurry temperature, the particles in the liquefy mixing procedure are consolidated over the liquid combination's liquids' temperature.

The vortex is used to display support particles in each of the two cycles. Nevertheless, there are two important problems with the dissolving system. First and foremost, as can be seen by comparing their thickness to that of the fluid metal, the ceramic particles frequently sink or float and are not wetted by the fluid metal framework. The ability of a fluid to spread over a strong surface is known as wettability, and it refers to the degree of intimate contact between the fluid and strong [A.R.I. Kheder et al., (2011)]. As a result, the composite has low mechanical qualities, large porosity, and an un favorable dispersion of the artistic particles. This deals with a fantastic test of mixing cast MMCs. Unfortunately, poor wettability indicates that the liquid network is unable to wet the support particles' outer layer; as a result, the particles essentially float on the surface, as evidenced by surface strain, a large surface area, high interfacial energy, and the existence of an oxide coating on the softening surface.

A number of techniques, such as mechanical blending, heating the particles to remove adsorbed gases from the molecule surface [S.A. Sajjadi et al., 2011], adding alloying components, using surface coatings on support molecules, and so on, can improve wettability to a certain extent [Zhiqiang.Y U, (2005)]. The dispersion of support particles in the liquid grid is an additional problem. Agglomeration and bunching of the particles will occur as a result of these particles' tendency to wander or become comfy in the liquid lattice due to the thickness difference between the grid and support [S.A. Sajjadi et al., 2011]. It has been determined that adding idle transporter gas to particles can help to accelerate the spread [S.A. Sajjadi et al., 2011]. In this way, developing a plan for making Al-MMCs that evaluate fuse and circulate supporting particles in the liquid lattice is crucial.

The goal of the current review is to use mix projecting method to combine 6061Al-Al_2O_3 particulate MMC. A unique three-phase blending method combined with preheating of the building particles is being adopted in order to further improve wettability and dispersion of supporting particles.

Experimental Details

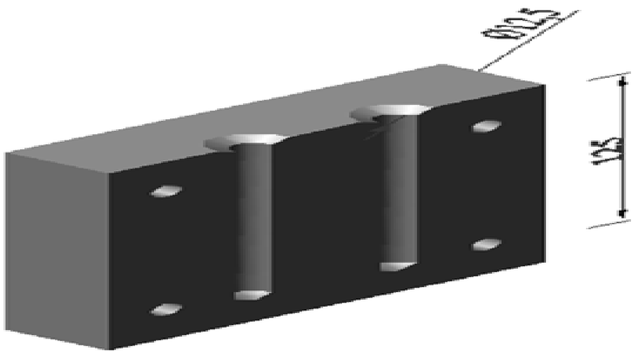

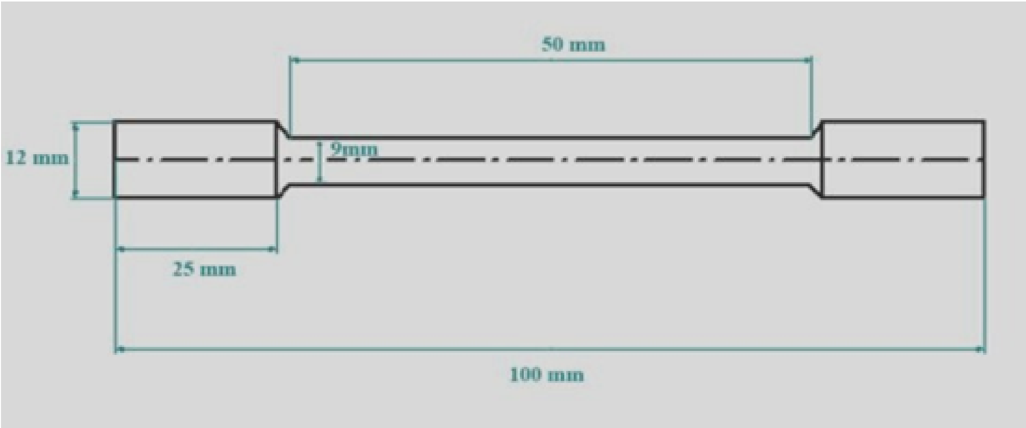

Figure.1showing the details of (a) Permanent mold for producing compo sites(b)Dimensions of the tensile specimen

6061Al-compound was the network material used for this evaluation. The artificial grid material arrangement, determined by means of an Atomic Absorption Spectrophotometer (model AA-670, Varian, The Netherlands), is presented in Table 1. Al_2O_3 particles measuring 135μm in size and with shifting measurements of 9, 12, and 15wt% are used as filler material while composites are being prepared. Composites have been planned using the mix projecting method. The initial measured measurement of 6061Al composite was poured into a SiC pot and heated in an electrical obstruction heater to 8500C. The temperature of the heater was precisely managed.Using an electronic temperature controller to help you reach 525℃. The building block particles are heated in conjunction with the initial three-phase mixing procedure. Fired Al_2O_3 particles were heated to 2100℃ in a stove in order to eliminate the adsorbed gases from the molecular surface and avoid a sudden drop in temperature after particulate expansion. Before heating Al_2O_3 particles were added to the liquid combination's vortex, strong hex chloral ethane (C2Cl6) was utilized to effectively degas the mixture. Vortex formation is aided by a zirconia-coated steel impeller.

The degree of Al_2O_3 particle joining in the framework compound was completed in three phases. As an example, the total quantity of help required was determined and is being added to the dissolve over time as opposed to all at once. For 10 minutes, mechanical mixing is completed after each support presentation. The stirrer, which was heated before being submerged in the liquefy, was found approximately two thirds of the way down the liquid metal from the base and was spinning at 200 rpm. At a pouring temperature of 7500℃, the composite material was poured into very durable cast iron molds measuring 125 mm in length and 12.5 mm in width.

The pre-assembled composites were represented by little studies. Using an optical microscope (Olympus model DS X100), samples of 12 mm in width and 10 mm in thickness were cut from the focus part of the projected picture for microstructural emphasis on led. A scanning electron microscope (made in Joel, Japan) was used to take SEM images. For an XRD (Philips scientific) inquiry, a plot of the power of the 2-theta stanzas may be examined using both starting and programming. The hypothetical thickness is obtained by determining the densities of the Al_2O_3 particles and the 6061Al network to be 2.7 and 3.9 gm/cm3, respectively. The thickness of the samples was estimated using Archimedes' technique. The mechanical behavior of the composites was investigated by performing hardness and malleability tests using Zwick and a modified unit-hub ductile testing equipment.

The components of the form are depicted in Fig. 1, together with a malleable inspection example. The Micro-Vickers hardness upsides of the composites were evaluated using the MVH-II computerized micro hardness analyzer (Zwick/Rowell indenter) with an Al_2O_3 particle heap of 20N. The average of 100 measurements taken at different points on the cleaned sample to determine the hardness value is given.

Malleable experiments were carried out in a similar manner when Al_2O_3 particles expanded. For every composite, three tests were administered, and normal worth was taken into account.

Table.1 presents the Al6061 alloy's chemical composition as determined by Varian, the Netherlands, using an atomic absorption spectrophotometer (Model AA-670).

Elements	**Mg**	**Fe**	**Si**	**Cr**	**Cu**	**Pb**	**Zn**	**Ti**	**Mn**	**Ni**	**Sn**	**Al**
Percentage	0.804	0.6	0.44	0.27	0.25	0.23	0.22	0.16	0.149	0.04	0.002	Balance

RESULTS AND DISCUSSIONS

Micro structural studies

Because of the extremely low wettability of alumina particles and agglomeration characteristics that result in non-uniform appropriation and poor mechanical qualities, creating metal-lattice composites with alumina particles by projection cycles is usually problematic.

The current study aims to plan Al6061 aluminum compound framework composites with small alumina particles by combining a three-phase blending process with mix projecting and preheating the supporting particles. The percentages of greatness alumina powder used in the composites were 7, 10, and 13 weight percent. Fig. 2(a-h) shows the optical micrographs of the 6061Al compound containing 0, 7, 10, and 13wt% Al_2O_3 particulates.

Fig. 2a-h shows microstructure of as cast 6061Al and 6061Al with 7 wt.% (Fig. 2c-d), 10wt% (Fig. 2e-f) and 13wt% (Fig. 2g-h) Al_2O_3 particulates. The microstructure of the pre-arranged composites contains essential □-Al dendrites and eutectic silicon, while Al_2O_3 particles are isolated at between dendritic districts and in eutectic silicon. The blending of liquefy when presenting particles has brought about breaking of dendrite molded structure into equiaxed structure, it works on the wettability and fuse of particles inside the dissolve and furthermore it causes to scatter the particles all the more consistently in the network.

Fig. 2c-h uncovers the dispersion of alumina particles in various examples and it very well may be seen that there is genuinely uniform appropriation of particles and furthermore agglomeration of particles at few spots were seen in the composites supported with 7wt%, 10wt% and13wt% Al_2O_3. The microphotographs likewise show that the Al_2O_3 particles have propensity to isolate and bunch at between dendritic districts which are encircled by eutectic silicon (Fig. 2c-h). Further, the micrographs show that grain size of the built up composite (Fig.2.a-h) is more modest than the amalgam without alumina particles (Fig. 2a-b) on the grounds that, Al_2O_3 particles added to dissolve likewise go about as heterogeneous nucleating locales during cementing.

SEM photos were gotten utilizing Scanning Electron Microscope (Make-Joel, Japan). Fig. 3(a-c) shows the SEM photos of 6061Al with 7 wt. %(Fig.3a), 10 wt. %(Fig.3b) and 13wt %(Fig.3c) Al_2O_3 particulates. Fig. 3c (13wt %) uncovers great dispersion of particles and extremely low agglomeration contrast with 9 wt. %(Fig.3b) and 13wt%(Fig.3c) Al_2O_3particulates. Moreover, the figure shows that the Al_2O_3 particles have inclination to isolate and group at between dendritic locales which are encircled by eutectic silicon (Fig.3a-c).

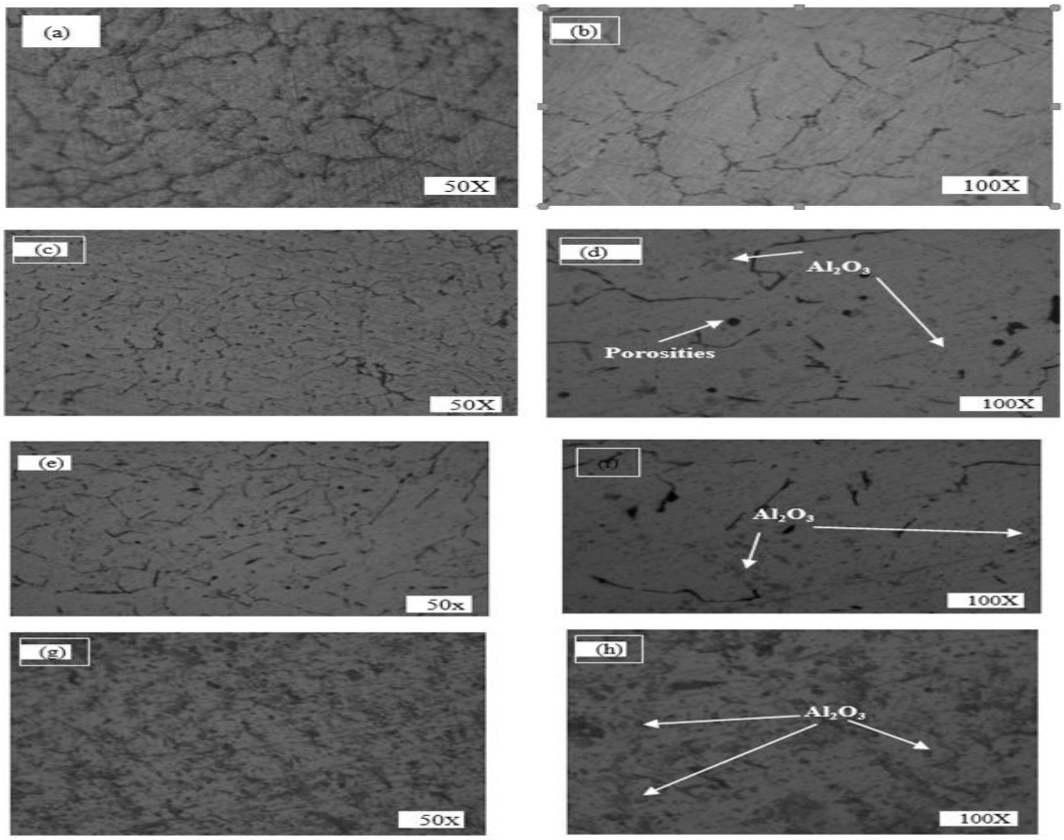

Fig.2ah Showing the optical micro photo graphs of 6061 Al with and without Al2O3 particulates at50X&100X(a-b)as-cast,(c-d)with 6wt % of Al2O3 p, (e-f) with 9wt% of Al $_2O_3$ p & (g-h)with12wt%ofAl_2O_3pat 100X.

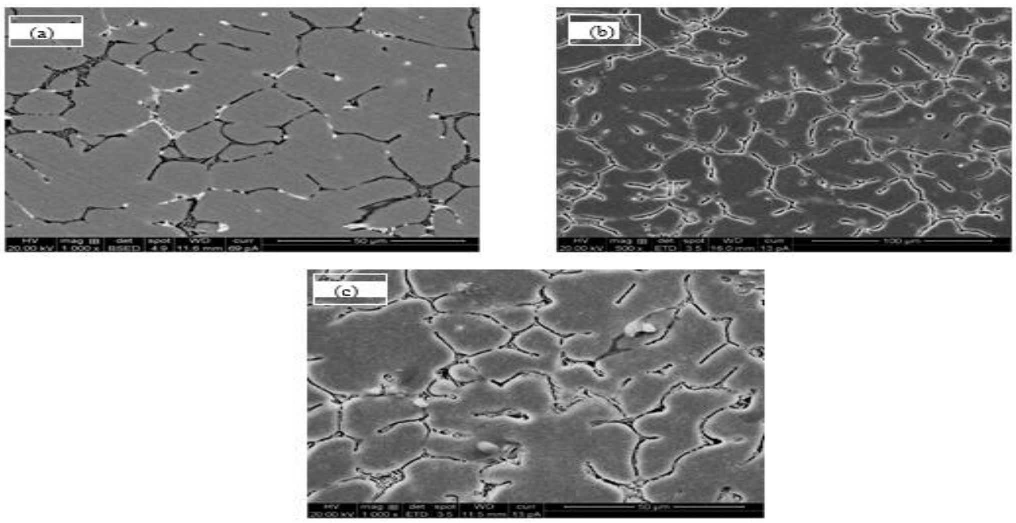

Fig.3-a-c showing the SEM photographs of 6061Al with Al_2O_3particulates (a) with7 wt. %ofAl_2O_3p, (b) with10wt%ofAl_2O_3p& (c) with 13wt%ofAl_2O_3

X-Ray Diffraction Analysis

Fig.3.1 (a-b) shows the XRD examinations were directed on 6061Al based composites supported with 8 and 13wt% of Al_2O_3particles to affirm the presence of Al_2O_3as to distinguish different stages shaped. Fig.3.1. a. Shows the X-beam diffraction example and consequences of 6061Al composite with 10 wt.% Al_2O_3MMC's.In X-beam diffraction design (Fig. 3.1.a), nine peaks have been gotten in the 3 range going from 25 to 110 and the tops at 2ɵ of 39.44°, 45.7°, 66.32° and 76.2°belongs to Pure Al and the tops at 2ɵ of 42.34°, 49.45°, 55.54° and 77.41° has a place with Al_2O_3 and other staying minor pinnacles credited to impurity. Fig.3.1. b. Shows the X-beam diffraction example and consequences of 6061Al amalgam with 13 wt.% Al_2O_3MMC's.In. In X-beam diffraction (Figure 3.1.b), Ten pinnacles have been gotten in the 3 range going from 25 to 110 and the tops at 2ɵ of 39.45 °,42.96°, 64.42°belongs to Pure Al and the tops at 2ɵ 27.42°, 38.57°, 45.75°, 59.3° and 67.3°belongs to Al_2O_3 and other excess minor peaks attributed to impurity.

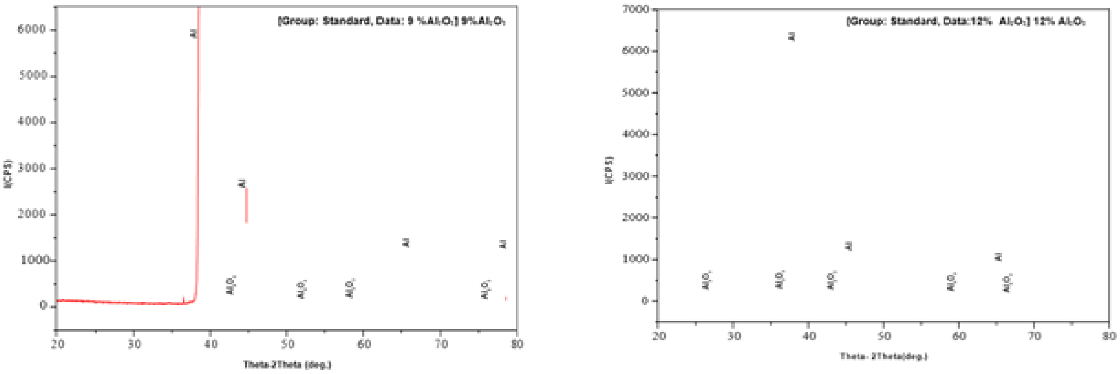

Fig.3.1showingtheX-ray diffraction pattern of the 6061 Alalloy with (a)7 wt.%$Al_2O_3$and(b) 10wt.%Al_2O_3 © 13wt.%Al_2O_3

Hardness measurements

Fig.3.2 shows the consequences of miniature hardness tests led on Al6061 combination and the 6061Al composite containing different weight level of Al_2O_3particles. The Micro-Vickers hardness were estimated on the cleaned tests utilizing jewel cone indenter with a heap of 20N and the worth revealed is normal of 100 readings taken at various areas. A critical expansion in hardness of the combination grid should be visible with expansion of Al_2O_3 particles. Higher worth of hardness is obvious sign of the way that the existences of particulates in the lattice have worked on the general hardness of the composites. This is valid because of the way that aluminum is a delicate material and the built up molecule particularly earthenware production material being hard, contributes decidedly to the hardness of the composites. The presence of stiffer and harder Al_2O_3 support prompts the expansion in imperative to plastic misshaping of the network during the hardness test. Subsequently increment of hardness of composites could be credited to the generally high hardness of Al_2O_3 itself.

Table.2: showing the theoretical and measured densities of as cast 6061Alandwith7wt.%, 10wt.%,

Composition	Theoretical Density (g/cm3)	Measured Density(g/cm3)
6061Al+7% Al_2O_3p	2.73	2.58
6061Al+10% Al_2O_3p	2.77	2.6
6061Al+13% Al_2O_3p	2.8	2.37

13wt. %, ofAl_2O_3prespectively

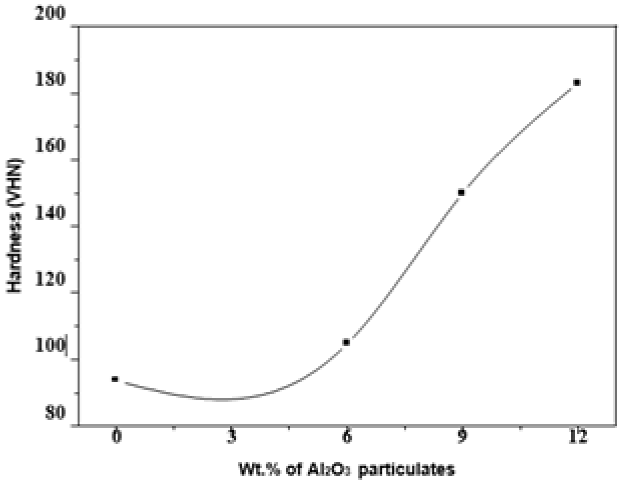

Fig.3.2Graph showing the variations in hardness of 6061 Al before and after addition of different wt.% of Al_2O_3particulates

Tensile Properties

To examine the mechanical way of behaving of the composites the elastic tests were completed utilizing automated unit-pivotal malleable testing machine according to ASTM norms. Three examples were utilized for each test and normal worth is accounted for. The tractable properties, for example, rigidity, yield strength and % lengthening were removed from the pressure strain bends and are addressed in Table 3.2. furthermore, Fig. 3.3a-b. From fig. obviously break strength of composites (7, 10 and 13wt %) is higher when contrasted with as cast 6061Al, while pliability of composite is lesser that unreinforced combination. It is additionally obvious from fig. that the rigidity increments with expansion in measure of support, while there is decline in flexibility with expanding measure of support. Expansion in strength is potentially because of the warm jumble between the metallic grid and the support, which is a significant component for expanding the separation thickness of the lattice and in this manner, expanding the composite strength. In any case, the composite materials showed lower lengthening than that of unreinforced examples. Clearly plastic misshaping of the blended delicate metal framework and the non-deformable support is more troublesome than the base metal itself. Subsequently, the pliability of the composite drops down when contrasted with that of unreinforced material.

Table.3.showing the tensile test results of ascast 6061 Al, with addition of7,10 and 13wt.%ofAl_2O_3particulatesto6061Al

Sl. No.	Weight percentage of Al_2O_3 particles (%)	Yield Stress (MPa)	Ultimate Tensile strength (MPa)	Extent of Improvement in UTS Value (%)
1	0	137.05	148.65	-
2	7	144.52	166.84	11.10
3	10	154.84	174.73	14.82
4	13	177.82	196.63	30.17

International Journal of Research Radicals in Multidisciplinary Fields (IJRRMF), ISSN: 2960-043X
Volume 2, Issue 2, July-December, 2023, Available online at: www.researchradicals.com

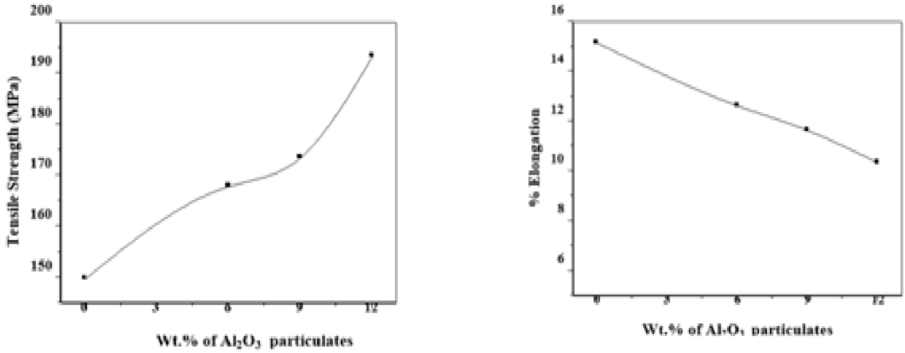

Fig.3.3Graphs showing the tensile test results of 6061Al-alloybeforeandafteradditionofAl_2O_3 particulates(a) Variation inultimate tensile strength (b) Variation in % elongation

Wear properties

A pin-on-plate tribometer is utilized to play out the wear try. The wear track, amalgam and composite examples are cleaned completely with CH3) 2CO preceding test. Every example is then weighed utilizing a computerized balance having an exactness of ±0.0002 gm. After that the example is mounted on the pin holder of the tribometer prepared for wear test. For all examinations, the sliding rate is changed in accordance with 2.366 m/s, track width 801mm, load 20.52N and complete time is 35 moments under room temperature. Fig.3.4 shows the aftereffects of the weight reduction led on 6061 Al combination and the 6061Al composite containing 0, 7, 10 and 13wt. % ofAl_2O_3 particles at a steady heap of 20.52N. From Fig.3.4 obviously weight reduction in the event of composites is diminished when contrasted with the base compound (6061 Al alloy). This is because of the molecule haul out, on account of composite supported alumina particles during wear test. Further expansion what's more degree of wt.% of support which diminishes the weight reduction of the composites. It is obvious from Fig.3.4 the most extreme weight reduction was seen in as cast 6061Al combination and least weight reduction was noticed for (6061Al compound +12%Al_2O_3). Fig.3.5 shows the consequences of wear rate (weight reduction) as a component of sliding distance for the 6061 Al compound and 6061Al composite containing 0, 7, 10 and 13wt. % Al_2O_3 of particles at a consistent heap of 20.52N and speed of 285 rpm. It is seen from the Fig.3.5 that wear pace of composites (7, 10 and 13wt %) diminishes after expansion of Al_2O_3 particles contrasted with base amalgam (6061 Al combination). This is because of the joining of hard Al_2O_3 particles in the 6061 Al compound limits such furrowing activity of hard steel partner and further develops the wear resistance. The results as shown from Fig.3.5 shows the diminishing pattern of wear rate with expansion in weight level of Al_2O_3 up to 15% weight division.

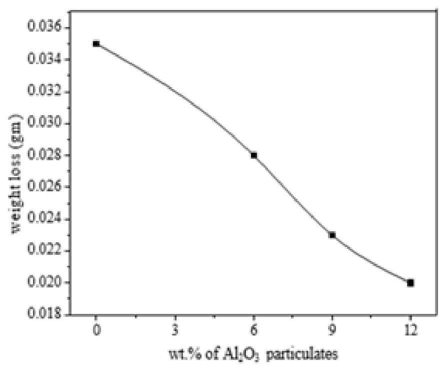

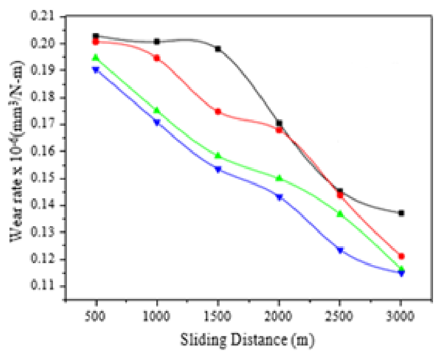

CONCLUSIONS

The current work on arrangement of 6061Al-Al_2O_3 metal framework composite by stir projecting and assessment of mechanical and wear properties has prompted following ends. The composites containing 6061Al with 7, 10 and 13wt% of Al_2O_3 particulates were effectively blended by soften mixing strategy utilizing three phases blending joined with preheating of the supporting particles.

The optical micrographs of composites delivered by mix projecting strategy shows genuinely uniform appropriation of Al_2O_3 particulates in the 6061Al metal grid. The microstructure of the composites contained the essential Al dendrites and eutectic silicon. While Al_2O_3 particles were isolated at between dendritic areas and in the eutectic silicon.

The hardness of the pre-arranged composites increments with increasing wt.% of Al_2O_3 particulates and Strength of arranged composites both tractable and yield was higher in the event of composites, while flexibility of composites was less when contrasted with as cast 6061Al. Further, with expanding wt.% of Al_2O_3, the elasticity shows a rising pattern.

Greatest weight reduction was seen in as cast 6061Al combination and least weight reduction was seen in 6061Al+13%Al_2O_3 composites at a consistent heap of 19.62 N and speed of 300 rpm and higher wear rate was seen in as cast 6061Al compound when contrasted with 6061Al-Al_2O_3 composites at a steady heap of 19.62N and speed of 300 rpm.

REFERENCES

[1]. Jawad Ahmad, Zhiguang Zhou, Ahmed Farouk Deifalla, “Structural properties of concrete reinforced with bamboo fibers”, Journal of materials research and technology, Volume 24, 844-865, 2023.

[2]. FadiAlthoey, Paul OluwaseunAwoyera, King Inyama, “Strength and microscale properties fiber-reinforced concrete modified with natural rubber latex”, Sec. Structural Materials, Volume 09, 2022.

[3]. Sravan Kumar Pala, Improving Customer Experience in Banking using Big Data Insights, International Journal of Enhanced Research in Educational Development (IJERED), ISSN: 2319-7463, Vol. 8 Issue 5, September-October 2020.

[4]. Bharath Kumar. (2022). Challenges and Solutions for Integrating AI with Multi-Cloud Architectures. International Journal of Multidisciplinary Innovation and Research Methodology, ISSN: 2960-2068, 1(1), 71–77. Retrieved from https://ijmirm.com/index.php/ijmirm/article/view/76

[5]. KarthikeyanKumarasamy, GShyamala, Haftom Gebreyowhanse, Harmanjeet Singh, “Strength properties of bamboo fiber reinforced concrete”, Materials science and engineering, Volume 04, 62-69, 2020.

[6]. Sravan Kumar Pala, Investigating Fraud Detection in Insurance Claims using Data Science, International Journal of Enhanced Research in Science, Technology & Engineering ISSN: 2319-7463, Vol. 11 Issue 3, March-2022.

[7]. Goswami, MaloyJyoti. "Study on Implementing AI for Predictive Maintenance in Software Releases." International Journal of Research Radicals in Multidisciplinary Fields, ISSN: 2960-043X 1.2 (2022): 93-99.

[8]. Bharath Kumar. (2022). AI Implementation for Predictive Maintenance in Software Releases. International Journal of Research and Review Techniques, 1(1), 37–42. Retrieved from https://ijrrt.com/index.php/ijrrt/article/view/175

[9]. Sunil Thakur, Kamal Kishore Thakur, Harmanjeet Singh, “A review paper on abrasive wear and tribology of graphite”, Source of AGU Int. J. Eng. Technol, Volume 04, 62-69, 2017.

[10]. M. Bindu, Dr. Narendra B.K, Manjunatha J.K, “A study on characteristic strength of bamboo reinforced concrete”, Materials science engineering, Volume 01, 2016.

[11]. Kaminski, S, Lawrence, A., & Trujillo, Design guide for engineered barbeque housing. INBAR–International Network for Bamboo and Rattan: Beijing, China, 2016.

[12]. Kaminski, S., Lawrence, A., & Trujillo, D. Structural use of bamboo: Part 1: Introduction to bamboo. The structural engineer, 94(8), 40-43, 2016.

[13]. SR Chauhan, Sunil Thakur, “Effects of particle size, particle loading and sliding distance on the friction and wear properties of cenosphere particulate filled vinyl ester composites”, Journal of Materials & Design , Elsevier, Volume 51, 398-408, 2013.

[14]. Goswami, MaloyJyoti. "Leveraging AI for Cost Efficiency and Optimized Cloud Resource Management." International Journal of New Media Studies: International Peer Reviewed Scholarly Indexed Journal 7.1 (2020): 21-27.

[15]. Neha Yadav, Vivek Singh, “Probabilistic Modeling of Workload Patterns for Capacity Planning in Data Center Environments” (2022). International Journal of Business Management and Visuals, ISSN: 3006-2705, 5(1), 42-48. https://ijbmv.com/index.php/home/article/view/73

[16]. Chintala, Sathishkumar. "Explore the impact of emerging technologies such as AI, machine learning, and blockchain on transforming retail marketing strategies." Webology (ISSN: 1735-188X) 18.1 (2021).

[17]. Ayyalasomayajula, M., and S. Chintala. "Fast Parallelizable Cassava Plant Disease Detection using Ensemble Learning with Fine Tuned AmoebaNet and ResNeXt-101." Turkish Journal of Computer and Mathematics Education (TURCOMAT) 11.3 (2020): 3013-3023.

[18]. MMTA SathishkumarChintala, “Optimizing predictive accuracy with gradient boosted trees infinancial forecasting” Turkish Journal of Computer and Mathematics Education (TURCOMAT) 10.3 (2019).

[19]. Chintala, S. "IoT and Cloud Computing: Enhancing Connectivity." International Journal of New Media Studies (IJNMS) 6.1 (2019): 18-25.

[20]. Goswami, MaloyJyoti. "Study on Implementing AI for Predictive Maintenance in Software Releases." International Journal of Research Radicals in Multidisciplinary Fields, ISSN: 2960-043X 1.2 (2022): 93-99.

[21]. Bharath Kumar. (2022). Integration of AI and Neuroscience for Advancing Brain-Machine Interfaces: A Study. International Journal of New Media Studies: International Peer Reviewed Scholarly Indexed Journal, 9(1), 25–30. Retrieved from https://ijnms.com/index.php/ijnms/article/view/246

[22]. Sravan Kumar Pala, Use and Applications of Data Analytics in Human Resource Management and Talent Acquisition, International Journal of Enhanced Research in Management & Computer Applications ISSN: 2319-7463, Vol. 10 Issue 6, June-2021.

[23]. Pala, Sravan Kumar. "Databricks Analytics: Empowering Data Processing, Machine Learning and Real-Time Analytics." Machine Learning 10.1 (2021).

[24]. Santram Chauhan, Sunil Thakur, “Effect of micro size cenosphere particles reinforcement on tribological characteristics of vinylester composites under dry sliding conditions”, Journal of Minerals and Materials Characterization and Engineering , Scientific Research Publishing, Volume 11, Issue 10, 938, 2012.

[25]. Sunil Thakur , SantramChauhan, , “Effect of micron and submicron size cenosphere particulate on mechanical and tribological characteristics of vinylester composites”, Journal of Proceedings of the

Institution of Mechanical Engineers, Volume 228, Issue 04, 415-423, 2012.

[26]. Goswami, MaloyJyoti. "Optimizing Product Lifecycle Management with AI: From Development to Deployment." International Journal of Business Management and Visuals, ISSN: 3006-2705 6.1 (2023): 36-42.

[27]. Vivek Singh, NehaYadav. (2023). Optimizing Resource Allocation in Containerized Environments with AI-driven Performance Engineering. International Journal of Research Radicals in Multidisciplinary Fields, ISSN: 2960-043X, 2(2), 58–69. Retrieved from https://www.researchradicals.com/index.php/rr/article/view/83

[28]. Sravan Kumar Pala, "Synthesis, characterization and wound healing imitation of Fe3O4 magnetic nanoparticle grafted by natural products", Texas A&M University - Kingsville ProQuest Dissertations Publishing, 2014. 1572860.Available online at: https://www.proquest.com/openview/636d984c6e4a07d16be2960caa1f30c2/1?pq-origsite=gscholar&cbl=18750

[29]. Sunil Thakur, SR Chauhan, "Optimisation of cutting parameters using Taguchi design of experiment for titanium alloy (grade-5) on CNC turning centre", International Journal of Machining and Machinability of Materials, Volume 12, Issue 04, 398-416, 2012.